

TIPP 2011 - Technology and Instrumentation for Particle Physics 2011

The ICARUS T600 detector at LNGS underground laboratory

N. Canci¹

*INFN - Laboratori Nazionali del Gran Sasso
S.S. 17 bis km 18+910
67010 - Assergi (AQ), Italy*

Abstract

ICARUS (Imaging Cosmic And Rare Underground Signals) is the the largest Liquid Argon Time Projection Chamber (LAr-TPC) in the world (containing ~600 tons of LAr) addressed to the study of rare events and, among these, neutrino interactions. Installed in the Gran Sasso National Laboratory (INFN-LNGS, Italy), ICARUS started working gradually since May, 27th 2010, collecting data both from the cosmic rays able to reach the depths of the laboratory and from neutrino interactions from the CNGS beam. The detector, providing a completely uniform imaging and calorimetry with a high accuracy on massive volumes, allows to reconstruct in real time neutrino and cosmic interactions, measuring the full kinematics of the identified particles. The ICARUS technology can be considered as a milestone towards the realization of next generation of massive detectors (tens of ktons) for neutrino and rare event physics.

In this paper a short description of the ICARUS T600 experiment, detector main features and performances and its first underground results are presented.

© 2012 Published by Elsevier B.V. Selection and/or peer review under responsibility of the organizing committee for TIPP 11. Open access under [CC BY-NC-ND license](https://creativecommons.org/licenses/by-nc-nd/4.0/).

Keywords: Liquid Argon, TPC, Noble Liquid detectors, Cryogenic Detectors, Particle tracking detectors, Neutrino interaction

1. Liquid Argon Time Projection Chamber detection technique

The Liquid Argon Time Projection Chamber (LAr-TPC), first proposed by C. Rubbia in 1977, is a powerful detection technique providing a 3D imaging of any ionizing event [1].

This continuously sensitive and self triggering detector is characterized by high resolution and granularity allowing for a precise reconstruction of events topology. The event reconstruction is completed by calorimetric measurement via dE/dx ionization signal over a very wide energy range, from MeV to several tens of GeV.

The operational principle of the LAr TPC is based on the fact that a charged particle interaction in LAr induces atomic excitation and ionization (electron-ion separation), followed by recombination; both processes lead to the emission of a narrow band luminescence UV photons. Therefore, ionization and scintillation emission are processes strictly connected. If an electric field is applied to the considered liquid Argon volume, part of the initially produced ionization can be collected (Fig. (1)) and, in principle, the

¹On behalf of the ICARUS Collaboration. E-mail: nicola.canci@lngs.infn.it

ratio between the collected light and charge could be used to discriminate the nature and the kinematical condition of the primary impinging particle [2, 3, 4].

Some liquid Argon main physical characteristics have been shown in Tab. (1).

Mean Energy Loss (mip)	$\langle dE_{mip}/dx \rangle = 1.519 \text{ MeVcm}^2/g$
Average Energy for (e^- , Ar^+) pair production	$W_{LAr} = 23.6 \text{ eV}$
Mean Electron Number/cm [@ 500 V/cm] (mip)	$N_e/cm \simeq 6 \cdot 10^4 \text{ e}^-/cm$
Ar_2^* excited dimer states (M-band)	Singlet $^1\Sigma_u$; Triplet $^3\Sigma_u$
Decay γ Energy	$\langle E_\gamma \rangle = 9.7 \text{ eV}$
Decay γ Spectrum	$\langle \lambda_{scint} \rangle = 128 \text{ nm}$; $\sigma_{scint} \simeq 3 \text{ nm}$
Decay Time constants	$\tau_S \sim 4 \div 6 \text{ ns}$; $\tau_T \sim 1.2 \div 1.6 \mu\text{s}$
Decay Intensity Ratio (mip)	$I_S/I_T = 0.3$ (23%/77%)
Average Energy for γ production	$W' = 19.5 \text{ eV}$
Photon Yield [@ 0-Field] (ideal)	$Y_\gamma = 5.1 \times 10^4 \text{ } \gamma/\text{MeV}$
[@ 0-Field] (mip)	$Y_\gamma \simeq 4.1 \times 10^4 \text{ } \gamma/\text{MeV}$
[@ 500 V/cm] (mip)	$Y_\gamma \simeq 2.4 \times 10^4 \text{ } \gamma/\text{MeV}$
Mean Photon Number/cm [@ 500 V/cm] (mip)	$N_\gamma/cm \simeq 5 \cdot 10^4 \text{ } \gamma/cm$
Rayleigh scattering length (@ 128 nm, 89 K)	$L_R = 90 \text{ cm} \pm 35\%$
Attenuation length (ultra-high purity)	∞
Refractive index @ 128 nm	1.38
Rayleigh scattering length	$\lambda_0 = 90.0 \text{ cm}$
Čerenkov photons per cm (110-600 nm)	1430 γ/cm
Electron Mobility (boiling point)	$500 \text{ cm}^2/V \cdot \text{s}$
Electron Drift Velocity [@ 500 V/cm](89 K)	$1.55 \text{ mm}/\mu\text{s}$
Electron Diffusion Coefficient (89 K)	$4.8 \text{ cm}^2/\text{s}$

Table 1. Liquid Argon main physical properties.

In highly purified LAr ionization tracks can be transported practically undistorted by a uniform electric field (typically 500 V/cm) over macroscopic distances: in fact, the low diffusion coefficient allows to have undistorted tracks for 1.5 m at least, thanks to the reduced wire pitch (usually of ~ 3 mm). Imaging is provided by a suitable set of electrodes (wires) placed at the end of the drift path continuously sensing and recording the signals induced by the drifting electrons [5].

Non-destructive read-out of ionization electrons by charge induction allows to detect the signal of electrons crossing subsequent wire planes with different orientation. This provides several projective views of the same event, hence allowing space point reconstruction and precise calorimetric measurement.

In particular, the measurement of the absolute time of the ionizing event, combined with the electron drift velocity information ($v_D \sim 1.6 \text{ mm}/\mu\text{s}$ at $E_D = 500 \text{ V/cm}$), provides the absolute position of the track along the drift coordinate. The determination of the absolute time of the ionizing event is accomplished by the detection of the prompt scintillation light produced in LAr by charged particles (5000 γ per mm of path at 500 V/cm) [6].

The high resolution and granularity of the LAr-TPC imaging allow precise reconstruction of events topology: particle identification is obtained through dE/dx versus range analysis and thanks to the decay/interaction topology. Electrons are identified by the characteristic electromagnetic showering; they can be well separated from π^0 via γ reconstruction, dE/dx signal comparison and π^0 invariant mass measurement at the level of permil: this feature guarantees a 90% efficiency identification of the leading electron in ν_e charged-current (CC) interactions, while rejecting neutral-current (NC) background to a negligible level [7]. Estimated energy resolutions for electromagnetic showers, hadronic showers and low energy electrons have been reported in Tab. (2).

For long muon tracks escaping the detector, momentum is determined exploiting their multiple scattering

by a Kalman filter algorithm with an average resolution $\Delta p/p \sim 15\%$, mainly depending on the track length [8].

Events	$\sigma(E)/E$
Electromagnetic Showers	$3\% / \sqrt{E(\text{GeV})}$
Hadronic Showers	$30\% / \sqrt{E(\text{GeV})}$
Low Energy Electrons	$(11\% / \sqrt{E(\text{MeV})}) + 2\%$

Table 2. Estimated energy resolutions for electromagnetic showers, hadronic showers and low energy electrons.

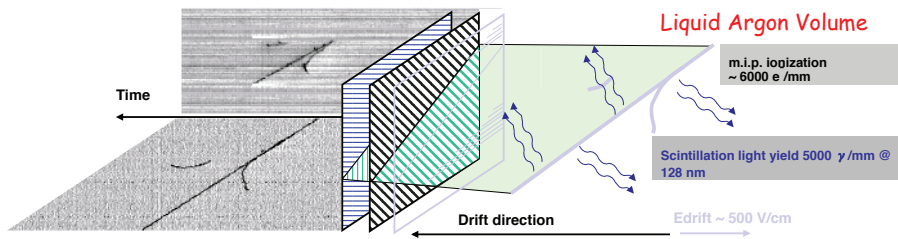


Fig. 1. Illustration of the LAr-TPC working principle: from a charged particle ionization path in LAr to its geometrical reconstruction.

2. The ICARUS T600 experiment

2.1. Detector overview

The ICARUS T600 detector consists of a large cryostat split into two identical, adjacent half-modules, with an overall volume of about 760 tons of ultra-pure liquid Argon at 89 K temperature (Fig. (2)) [9]. Each half-module, with internal dimensions $3.6 \times 3.9 \times 19.6 \text{ m}^3$, houses two Time Projection Chambers (TPC) separated by a common cathode. Each TPC is made of three parallel wire planes, 3 mm apart, oriented at 0° and $\pm 60^\circ$ w.r.t. the horizontal direction: in total 53248 wires, with length up to 9 m, are installed. By appropriate voltage biasing, the first two planes (Induction-1 and Induction-2 planes) are transparent to drift electrons and measure them in a non-destructive way, whereas the ionization charge is finally collected by the last one (Collection plane). The application of an electric field $E_D = 500 \text{ V/cm}$, kept uniform by appropriate eld shaping electrodes, ensures that the 1.5 m maximum drift distance is covered in 1 ms. The signals coming from each wire are continuously read and digitized at 25 MHz ($\sim 400 \text{ ns}$ t-sample) and recorded in multi-event circular buffers. The detection of the prompt scintillation light is also necessary to determine both the absolute time of the ionizing events and the trigger signal. For this purpose arrays of Photomultiplier Tubes (PMTs), operating at the LAr cryogenic temperature and made sensible to VUV scintillation light (128 nm) by applying a wavelength shifter layer (TPB), are installed behind the wire planes.

2.2. Cryogenic plant

One thermal insulation layer surrounds the two half-modules: it is realized by evacuated honeycomb panels assembled to realize a tight containment vessel [9]. Between the insulation and the aluminum containers a thermal shield is placed, with boiling Nitrogen circulating inside, to intercept the heat load and maintain the cryostat bulk temperature uniform (within 1 K) and stable at 89 K. Nitrogen used to cool the T600 half-modules is stored in two 30 m^3 LN_2 tanks positioned at the top of the plant. Its temperature is fixed by the equilibrium pressure in the tanks ($\sim 2.1 \text{ bar}$, corresponding to about 84 K), which is kept stable in steady state by a dedicated re-liquefaction system of 12 cryocoolers (48 kW global cold power),

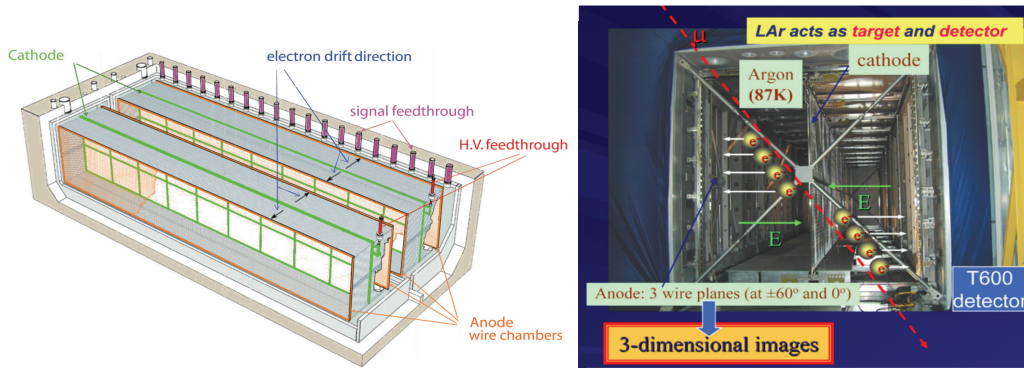


Fig. 2. Scheme of the detector [Left] and a picture of the LAr TPC with an artistic view of the working principle [Right].

thus guaranteeing safe operation in closed-loop. The two half-modules were cooled down to 90 K in ~ 8 days, while injecting of ultra-pure Argon gas to ensure uniform temperature throughout the whole detector. Cryostats were filled in parallel with commercial LAr, purified in-situ before entering the detector, at a rate of $\sim 1\text{m}^3/\text{hour}$ per cryostat with 47 trucks in about 2 weeks for a total amount of 610511 Argon liters. During the whole period the four gaseous re-circulation systems were operating at maximum speed to intercept the degassing impurities. In steady state the cryogenic plant is operating in closed loop maintained smoothly in stable conditions by the installed cryo-coolers. One month after filling, the forced liquid argon recirculation and purification started on both cryostats at rate of $1\text{m}^3/\text{hour}/\text{cryostat}$. In Fig. (3) an artistic view and some pictures of the cryogenic plant have been reported.

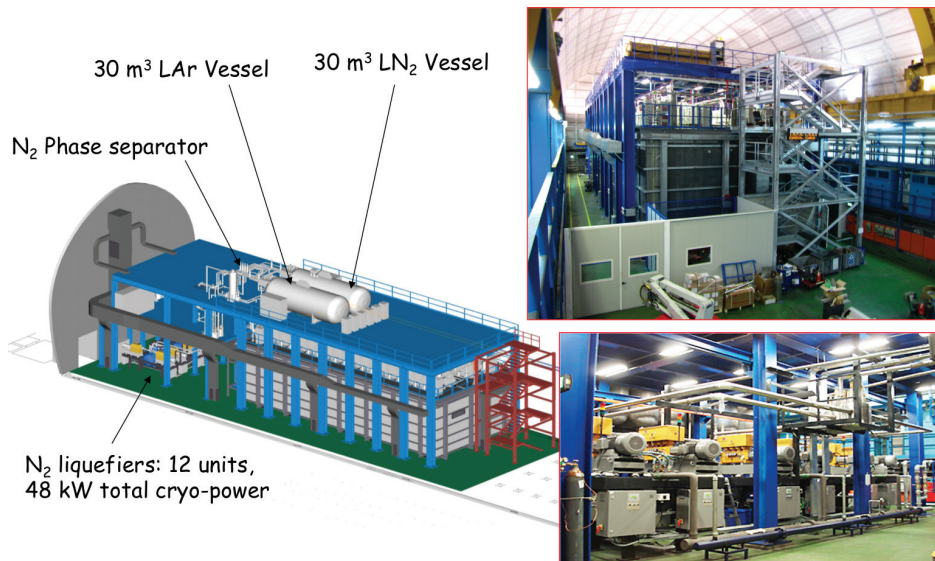


Fig. 3. Artistic view of the whole ICARUS T600 plant [Left]. ICARUS T600 detector in the Hall B of the LNGS underground laboratory [Right].

2.3. LAr purity and purification

A fundamental requirement for the performance of the liquid argon TPC is that electrons produced by ionizing particles can travel unperturbed from the point of production to the collecting planes. To this end

impurities in the liquid must be reduced to a very low level. In order to ensure stable performance of the device, the purity must be preserved in the dewar hosting the inner detector for the longest possible period of time. The major electronegative impurities in LAr are (electron attaching) O_2 , H_2O , CO_2 and/or fluorinated or chlorinated compounds [10]. To achieve long electron drift paths the liquid must be free of these impurities, which will otherwise decrease the electron collection efficiency. To reach a negligible attenuation over the full drift distance, the concentration of impurities must be kept at the level of less than 0.1 part per billion (ppb) oxygen equivalent. Standard commercial LAr has a much higher contamination (typically a few parts per million oxygen equivalent); moreover, LAr can be contaminated inside the cryostat from outgassing of the walls and TPC components (electrodes, cables, PMTs, etc.). The required purity is therefore achieved with the help of a continuous purification of the Argon via the method of recirculation.

To this purpose, each half-module is equipped with two gas-argon and one liquid-argon recirculation/purification systems. Argon gas is continuously drawn from the cryostat ceiling and, re-condensed, drops into OxisorbTM filters to finally return to the LAr containers [11]. LAr instead is recirculated by means of an immersed, cryogenic pump ($\sim 2 \text{ m}^3/\text{h}$, full volume recirculation in 6 days) and is purified through standard Hydrosorb/OxisorbTM filters before being re-injected into the cryostats. To ensure an acceptable initial LAr purity, before filling, the cryostats were evacuated in order to perform an appropriate outgassing of the cryostat internal walls and all the detector materials. The vacuum phase lasted for three months. The residual pressure was lower than 10^{-4} mbar, mainly due to water vapor, which freezes on the internal walls during the subsequent detector cooling down phase, not affecting the LAr purity. The Oxygen contribution was measured to be at most 10% of the total pressure.

The electron lifetime is directly related to the impurity concentration by an inverse linear relationship; in fact, electron attachment processes to electro-negative impurities S are active:



whose reaction constant k_e can be expressed as follows:

$$k_e = \int \sigma(E)f(E)dE \quad (2)$$

where E is the electron energy, $\sigma(E)$ the process cross section and $f(E)$ the Maxwell-Boltzmann function for electrons [12, 10].

Under the assumption that the free electron concentration N_e produced by ionizing events is smaller than the impurity concentration N_S , the free electron concentration decreases in time as:

$$\frac{dN_e}{dt} = -k_e N_e N_S \implies N_e(t) = N_e(0)e^{-t/\tau_e} \quad (3)$$

where $N_e(0)$ is electron concentration at $t = 0$ while the *electron lifetime* τ_e is defined as:

$$\frac{1}{\tau_e} = k_e N_S \quad (4)$$

and represents the time after which the number of survived electrons reduces by a factor $1/e^2$. The lifetime estimation thus provides a direct measurement of the LAr impurity content and on other hands, its value is used to correct the electron charge lost during the drift path in the tracks reconstruction.

To this aim, the electron lifetime is continuously monitored studying the attenuation of the charge signal as a function of the drift time along clean through-going muon tracks in Collection view, i.e. straight tracks without clear δ -rays and associated γ 's; the negative signal induced by the PMTs on the wires marks the time at which the track entered the detector (Fig. (4)). About 50 muon tracks are sufficient to daily measure

²The value of the *rate constant* k_e obviously depends on the drift field applied to the active LAr volume. Reference value for O_2 at $E_d = 1 \text{ kV/cm}$ is $k_e = 5.5 \times 10^{10} \text{ lt moles}^{-1} \text{ s}^{-1}$ (equivalent to $1.9 \text{ ppm}^{-1} \mu\text{s}^{-1}$)³ and hence a lifetime of the order of 3 ms in Argon can be achieved with a total amounts of impurities $\sim 0.1 \text{ ppb}$.

the electron charge attenuation within a 3% precision, dominated by residual Landau charge fluctuations. With the liquid recirculation turned on, the LAr purity steadily increased, reaching values of free electron lifetime (τ_e) exceeding 6 ms in both half-modules after few months of operation (Fig. 5). This corresponds to 0.05 ppb O_2 equivalent impurity concentration, producing a maximum 16% charge attenuation, at the maximum 1.5 m drift distance.

The evolution of the residual impurity concentration can be described with a simple model as:

$$dN(t)/dt = -N/\tau_R + k_L + k_D \cdot \exp(-t/\tau_D) \tag{5}$$

where τ_R is the time needed to recirculate a full detector volume, k_L is the total impurity leak rate and degassing rate and k_D is the internal residual degassing rate assumed to vanish with a time constant τ_D . Uniform distribution of the impurities throughout the detector volume is also assumed, as experimentally supported by the lifetime measurement with muon tracks in different regions of the TPCs [13].

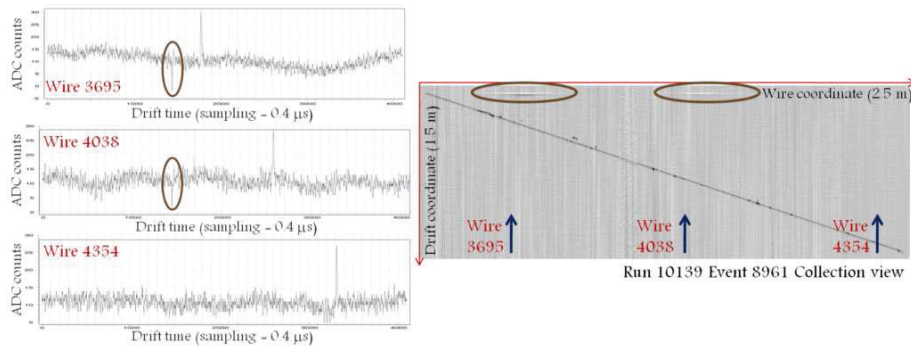


Fig. 4. A muon track candidate for the purity measurement [Right] and three different wire signals [Left] in Collection view. The $t=0$ signal, induced by PMTs on the wires, are circled. .

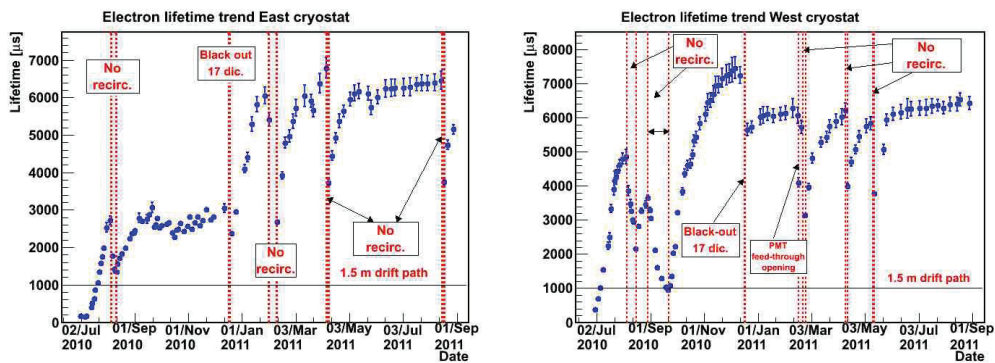


Fig. 5. Liquid Argon purity measurements for both the East [Left] and West [Right] cryostats.

3. T600 physics potential

3.1. 2010 physics run

ICARUS T600 started its operation in May 2010, collecting right from the beginning both cosmic rays and CNGS neutrino events. The trigger system relies on the scintillation light signals, with a starting layout

based, for each of the four TPC chambers, on the analog sum of signal from PMTs with a 100 photoelectron discrimination low threshold. The trigger for cosmic rays exploits the coincidence of the PMTs sum signals of the two adjacent chambers in the same half-module, relying on the 50% transparency of the cathode mechanical structure: this allows an efficient reduction of the spurious signals maximizing the detection of low energy events. An overall acquisition rate of ~ 50 MHz has been achieved well below the maximum allowed DAQ rate, resulting in about ~ 100 cosmic events per hour.

For CNGS neutrino events the proton extraction time information is also available, since an early warning signal is sent from CERN to LNGS 80 ms before the first proton spill extraction. Thus, accounting for the CNGS SPS cycle structure, i.e. two spills 50 ms apart and lasting $10.5 \mu\text{s}$ each, a dedicated trigger strategy has been chosen for the CNGS neutrino interactions, based on the presence of the PMT signal within a $\sim 60 \mu\text{s}$ gate opened in correspondence to the predicted extraction times delayed by the neutrino time of flight (2.44 ms) from CERN to LNGS.

A trigger rate of about 1 MHz is obtained, including neutrino interactions inside the detector and muons from neutrino interactions in the upstream rocks.

The CNGS run started in stable conditions on October, 1st 2010 and continued till the beam shutdown, on November, 22nd 2010; in this period 5.8×10^{18} proton on target (pot) were collected out of the 8×10^{18} delivered by CERN, with a detector lifetime up to 90% since November 1st (Fig. (6) [Left]). The 78% of the whole collected sample of events, corresponding to 4.52×10^{18} , has been preliminarily analyzed: 94 ν_{μ} CC and 32 NC events have been identified by means of visual scanning, while 6 events need for further analysis to be classified (being at edges, with μ track too short do be visually recognized); this result is in full agreement with the number of interactions predicted in the whole energy range up to 100 GeV ($2.6 \nu_{\mu}$ CC + 0.86ν NC) $\times 10^{-17}$ pot), to be corrected for fiducial volume and DAQ dead time. The analysis of the time distributions of this event sample, compared with the CNGS proton extraction time, allows to reconstruct the $10.5 \mu\text{s}$ spill duration, suggesting an good precision in the events timestamp (Fig. (6) [Right]).

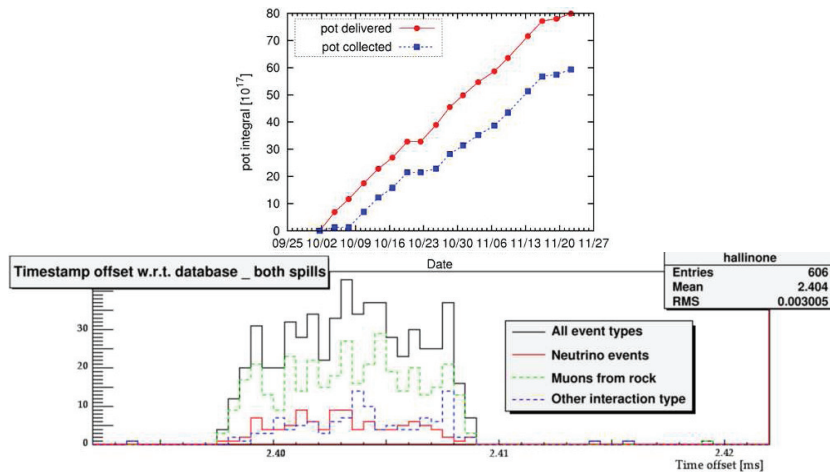


Fig. 6. Number of p.o.t. collected by ICARUS T600 in the Oct. 1st - Nov. 22nd run compared with the beam intensity delivered by CERN [Left]. Distribution of the difference between the neutrino interaction timestamp and the corresponding CNGS proton extraction time [Right].

3.2. Observation and reconstruction of neutrino events

The T600 at LNGS is detecting neutrino interaction events both from the CNGS beam and from cosmics. The neutrino interaction events are then fully 3D reconstructed: muons, pions, protons and kaons are identified by studying the event topology and the energy deposition per track length unit as a function of the

³3D track reconstruction starts from a 2D track finding algorithm based on an automatic clustering over an angle-position matrix; an approach based on principal curve analysis has been developed for three dimensional reconstruction.

particle range (dE/dx versus range) with a dedicated reconstruction program based on the polygonal line algorithm and on neural network. Electrons are recognized by the characteristic electromagnetic showering. Momentum of long muon tracks escaping the detector is determined by multiple scattering. An example of a ν_μ CC candidate real data event is shown in Fig. (7). The long muon track, about 13 meters, is impressive. The leading muon deposits by ionization a total energy of about 2.7 GeV before exiting the detector. The total hadronic energy in the event, $E_h = 2.3 \pm 0.5$ GeV, is certainly underestimated, since one particle from the secondary vertex escapes from the bottom side of the detector, and neutrons may have been produced and escaped detection.

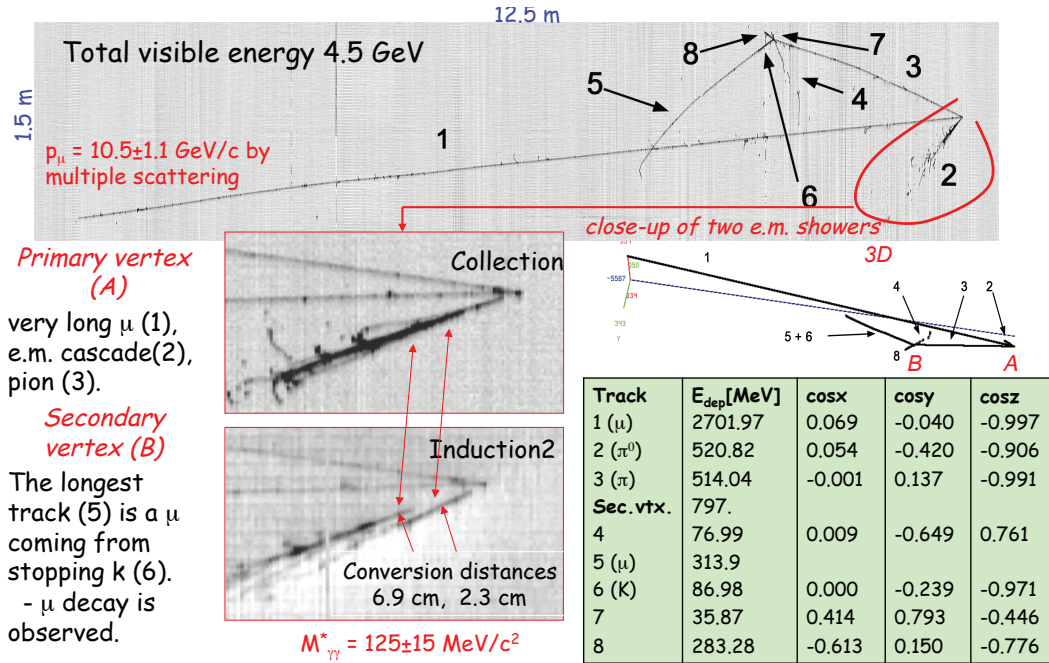


Fig. 7. An example of ν_μ CC interaction from the CNGS beam in the ICARUS T600 detector.

3.3. 2011-2012 CNGS run: physics perspectives

ICARUS T600 detector smoothly started data taking on March, 18th 2011 receiving the CNGS neutrino beam operating in high intensity dedicated mode. In the time interval from March 18th to May 23th CNGS delivered 1.7×10^{19} pot. The detector lifetime in the same period was about 93%, allowing the collection of about 1.5×10^{19} pot. The analysis tools to fully reconstruct the event topology and kinematics are under deployment with the real data, addressing in particular the main items of physics with the CNGS beam, i.e. ν_τ search, ν_e CC identification/measurement and NC rejection capability. A consistent analysis framework unifying all the available tools and allowing to store and share analysis results together with successive renements by different groups is also being finalized. It is expected to integrate as much as 10^{20} pot with the CNGS run in 2011-2012. For 1.1×10^{20} pot (including the data taken in 2010) about 3000 beam related muon neutrino CC events are expected in the ICARUS-T600. About 7 ν_e CC ($E_{\nu_i} > 20$ GeV) intrinsic beam associated events are also expected. Taking into account the $\nu_\mu \rightarrow \nu_\tau$ oscillation probability and the τ decay branching ratio into ν_e , a sufficiently clean separation from intrinsic ν_e CC events will result in 1-2 ν_τ CNGS events expected in ICARUS T600 in next 2 years. On the same beam, the search for sterile neutrinos in LNSD parameter space can be also performed, looking at an excess of ν_e CC events. ICARUS T600 is studying also neutrinos from natural sources (atmospheric, solar, supernovae) and it can play an interesting role in the nucleon decay search, in particular in interesting exotic channels not accessible to Čerenkov

detectors. With an exposure of a few years, its sensitivity on some supersymmetric favored nucleon decay channels will exceed the present known limits.

4. Conclusions

The ICARUS T600 detector, installed underground at the LNGS laboratory, is taking data since May 2010. The successful assembly and operation of this LAr-TPC is the experimental proof that this technique is mature. It demonstrates to have unique imaging capability, spatial and calorimetric resolutions and the possibility to efficiently distinguish electron from π_0 signals, thus allowing to better reconstruct and identify events with respect to the other neutrino experiments. This experiment address a wide physics programme. The main goal is to collect events from the CNGS neutrinos beam from CERN-SPS to search for the $\nu_\mu \rightarrow \nu_\tau$ oscillation and LSND-like ν_e excess, but also to study solar and atmospheric neutrino and explore in a new way the nucleon stability, in particular channels beyond the present limits. Furthermore, ICARUS T600 is a major milestone towards the realization of future massive LAr detector.

References

- [1] C.Rubbia, CERN-EP/77-08 (1977).
- [2] P. Benetti et al., Nucl. Instr. and Meth. A 332 (1993) 395.
- [3] P. Cennini, et al., Nucl. Instr. and Meth. A 345 (1994) 230.
- [4] P. Cennini et al, Nucl. Instr. and Meth. A 432 (1999) 240 - 248.
- [5] F. Arneodo, et al., Nucl. Instr. and Meth. A 449 (2000) 36.
- [6] P. Benetti et al., Nucl. Instr. and Meth. A 505 (2003) 89 - 92.
- [7] A. Ankowski et al., Acta Phys. Polon. B41 (2010) 103.
- [8] A. Ankowski et al., Eur. Phys. J. C48 (2006) 667.
- [9] S. Amerio et al., Nucl. Instr. and Meth A 527 (2004) 329 - 410.
- [10] A. Bettini, et al., Nucl. Instr. and Meth. A 305 (1991) 177.
- [11] P. Benetti, et al., Nucl. Instr. and Meth. A 333 (1993) 567.
- [12] G. Bakale et al., J. Chem. Phys. 80 (1976), 2556.
- [13] S. Amoroso, et al., Nucl. Instr. and Meth. A 516 (2004) 68.